



Scholars Research Library

Der Pharma Chemica, 2011, 3 (6):10-27
(<http://derpharmachemica.com/archive.html>)



ISSN 0975-413X
CODEN (USA): PCHHAX

Preparation and characterization of novel antibacterial nano-ceramic-composites for bone grafting

Hanan. H. Beherei^{1,3}, A. El-Magharby^{2,3}, M.S. Abdel-Aal^{1,3}

¹Physics Department, Science Faculty, Taif University, Taif state, KSA and Biomaterials Department National Research Center, Dokki, Tahrir st. Egypt

²Chemistry Department, Faculty Science, Taif University, Taif State, KSA

³Ceramic Department, Physics Department, National Research Center, Dokki, Tahrir st. Egypt

ABSTRACT

Novel nanocomposites scaffolds were prepared by impregnating nano-calcium phosphate (HA)/walled carbon nanotube (MWCNT)/ZnO nano-particles into the alginate polymers matrix. The nano-composite materials were characterized using X-ray diffraction (XRD), Fourier Transform Infrared (FT-IR) analyses mechanical test and Scanning Electron Microscopy (SEM) before in-Vitro and antibacterial test. The in-vitro behavior was assessed via measurement of calcium and phosphorus ions in SBF (simulated body fluid). FT-IR and SEM of the composites were performed pre and post immersion in SBF. The results prove that the bone like apatite layer formation was enhanced on the biopolymeric composite surface more than that on the polymeric composite containing more MWCNT. Therefore, the data confirmed that MWCNT plays an important role in the enhancement of the apatite formation. The conclusions proved that the MWCNT /polymeric biocomposites, containing more of MWCNT, are promising for antibacterial and bone remodeling applications.

Key words: Composite materials; Antibacterial biolymers; MWCNT; mechanical, pore analysis; analysis; *In-vitro*.

INTRODUCTION

Biomaterials have become indispensable for relieving pain and restoring biological functions to the attacked or the damaged parts of the body. The progressive deterioration of tissue with aging implied the innovation and development of highly modified spare parts for the body. Bone is especially vulnerable to fracture in senile people and in postmenopausal women as a result of loss of bone strength and bone density (osteoporosis) with aging or through hormonal depletion in postmenopausal or ovariectomized women.

With increasing population all over the world, there becomes a growing demand for highly efficacious biomedical materials which are capable to survive for 10 – 20 years longer than the traditional lean biomaterials.[1] Biomedical and bioengineering scientists have devoted condensed efforts for the production of a new generation of modern biomaterials that can perfectly withstand in surgical operations for repair and regeneration of damaged tissues. Molecular control over the texture and the rate of dissolution of bioactive materials paved the way to the production of novel biomaterials that can resorb at the same rate at which new trabecular bone is formed, whereas the mechanical properties of the regenerated trabecular bone are similar to those of the normal host bone. Noteworthy, optimizing the bioactive regenerative behavior, through modification and extension of the biomimetic research, offers great promise for producing a new generation of biomaterials that can enhance the repair, proliferation and regeneration of deteriorated bone tissues.[2-4] Some promising nano-materials for tissue replacement and regeneration will be obtained. On the basis of past experience and newly gained knowledge, nano-materials with tailored mechanical and biological performance can be manufactured and used to meet various clinical requirements. So, development of innovative multi-functional smart nano-materials should have a major impact in future applications.[5 and 6]

Hydroxyapatite (HA) is one of the bioceramics with higher bioactivity, but it has lower mechanical property than human load-bearing bone and its low dependability needs to be strengthened and toughened. If CNTs and HA were compounded we may obtain a composite with higher mechanical property and better biocompatibility.[7]

The study of CNTs composite has become one of the most interesting research topics. The composite with CNTs such as CNTs/ceramic [8] and CNTs/polymer [9 and 10] has been prepared, but a few studies about CNTs/ceramic composite and its security have been reported.

Carbon nanotubes (CNTs) should be ideal candidates for bone bioengineering because of their high strength and flexibility. Current medical treatments for bone defects generally involve replacement of lost bone with an artificial material. [11] Tissue engineering offers the chance to re-grow missing bone by culturing new cells on synthetic scaffolds or live prostheses. Unlike many potential bone scaffold materials, CNTs are not biodegradable. [12] A nanotube scaffold would consequently provide an inert platform on which cells could proliferate and deposit new living bone material.

Alginate, a polysaccharide derived from brown seaweed, has been widely utilized as cell carriers due to the simplicity for fabricating cell-immobilized beads or 3D porous scaffolds, low price compared to proteins or other natural polymers and non-toxicity to cells. It is also approved by the Food and Drug Administration (FDA) to human use as wound dressing material and food additive. The alginate, the monovalent salt form of alginic acid is a linear block copolymer composed of β -D-mannuronate (M-block) and α -L-guluronate (G-block) linked by 1,4-glycoside linkage. [13] The G-block of alginate has correspondingly high affinities for divalent ions such as calcium (Ca^{2+}), strontium (Sr^{2+}) and barium (Ba^{2+}) at room temperature and thus in an aqueous solution of divalent ions, the alginate chains are rapidly cross-linked *via* the stacking of G-blocks to form an egg-box structure and subsequently become gel. The 3D porous alginate scaffolds are usually fabricated by freeze-drying of the calcium-cross-linked gel. [14] The

hydrophilic nature of the alginate scaffolds allows simple and rapid cell seeding and the seeded cells maintain their viability and functions in culture. Although alginate, as well as other natural polymers, shows better biocompatibility than synthetic polymers, their practical applications for porous cell scaffolds are limited due to their brittleness or lack of flexibility. The alginate scaffolds also show poor adhesion to anchorage-dependent cells.

On the other hand, a well known issue in surgery and in particular as far as orthopedic surgery is concerned, is the development of infections, due to bacterial colonization of implanted materials. Though the discovery of antibiotics and the introduction of controlled hygienic protocols have remarkably minimized the risk of bacterial contamination during surgery and have decreased the danger of infection (2.5% in musculoskeletal surgery) [14], bacterial contagions can cause implant failure, prolong times and costs of hospitalization, and sometimes lead to patient's death. [15] Moreover, in the last years, many nosocomial bacteria have shown an increasing selective resistance towards antibiotics, inhibiting the efficacy of preventive antibiotic prophylaxes. [16] For instance, some micro-organisms are able to create a continuous slime, called biofilm, i.e. an extracellular polymer matrix consisting of glycoproteins and polysaccharides secreted by the bacteria themselves, which protects the micro-organisms. Antibiotics are often unable to penetrate inside the biofilm and so bacteria adhered to the biomaterials surfaces can proliferate undisturbed. The first step of bacteria colonization (the adhesion) is the most important event of biomaterials microbial infection and it is closely connected to surfaces nature; several surface treatments on biomaterials have been realized to decrease the risk of bacteria colonization. In particular, many antimicrobial agents have been used to modify the surface of biomaterials and attain antibacterial properties. [17]

These studies investigated the antibacterial activity of ZnO particles against *Escherichia coli*, *Salmonella typhimurium*, *Bacillus subtilis*, and *Staphylococcus aureus* etc. and the main conclusions of these studies can be summarized as the mechanisms of the antibacterial activity of ZnO particles are not well understood although Zhang, et.al.[18] proposed that the generation of hydrogen peroxide be a main factor of the antibacterial activity, and indicated that the binding of the particles on the bacteria surface due to the electrostatic forces could be a mechanism. It is shown that Zn has direct specific proliferative effect on osteoblastic and a potent and selective inhibitory effect on osteoclastic bone resorption. [19]

The ideal bone graft must be compatible, a scaffold for new bone formation, resorbable in the long-term, easy to manipulate, not support growth of pathogens, nonallergenic, available in particulate and molded forms, readily available, mechanically compatible with bone tissues. [20] The combination of polymers with nano-materials displays novel and often enhanced properties compared to the traditional materials. They can open up possibilities for new technological applications. It is one of today's challenging tasks to manufacture new multifunctional smart materials that possess intelligence at the material level.

In our work, nano-composites of carbon nanotubes, nano-hydroxyapatite and antimicrobial nano-ZnO with alginate will be synthesized. Microstructure characterization and morphology analysis on the nano-composites will be conducted using scanning electron microscope (SEM), mechanical properties, X-ray diffractometer (XRD), and fourier transform infrared spectrometer (FT-IR). The bone-bonding ability (bioactivity test in vitro) of nano-composites will be

evaluated by examining the ability of apatite to form on its surface in a simulated body fluid (SBF) with ion concentrations nearly equal to those of human blood plasma. However, the validity of this method for evaluating bone-bonding ability will be assessed systematically. It was concluded that examination of apatite formation on nano-composites in SBF is useful for predicting the in vivo bone bioactivity of a material.

MATERIALS AND METHODS

2.1. Materials

The polymer material used in this study was Alginate. Alginic acid sodium salt from brown algae with medium viscosity (weight-average molecular weight (*M_w*) 900 kDa) was purchased from Sigma. The starting material used in this method to prepare the composites was citric acid (Sigma).

HA powders were prepared by a wet chemical synthesis technique, based on the precipitation of HA nano-particles from aqueous solutions [21]. 136g of zinc chloride dehydrate is added to 450 ml of ethylene glycol, stir about for 20 : 30 minutes under 60 °C to prepare 500ml of 2M inorganic acidic was added. At the same time, 80 g of sodium hydroxide is added to 960 ml of water containing ethylene glycol and pH 9. The precipitate dried at 80°C and heated at 700°C. [22]

2.2. Preparation of Nano-composites

We prepared nano hydroxyapatite and nano-ZnO with carbon nanotube as filler powders and their loading onto alginate polymeric matrix as follow:

- 1- HA/Alginate composite.
- 2- HA/ZnO/Alginate composite (with ratio 2:1 of HA : ZnO).
- 3- HA/ZnO/ MWCNT /Alginate composite (with ratio 2:1 :1 of HA : ZnO: MWCNT)

Fixed weight (1.5 g) of filler nanopowders were dispersed, well mixed with the polymer mixture after 2.5 h from polymerization process from the previous experiment and kept at 40 °C in water bath for 30 min to complete the polymerization process in the presence of the filler. The nanopowders/alginate composites were left overnight at room temperature and then the mixture was washed with hot ethanol with stirring for 2 h. The composite mixture was filtered, collected and dried at 60°C overnight.

The composite scaffolds were prepared through the solid–liquid phase separation. Solvent extraction was chosen to remove the crystals after phase separation processes. A 12.5% wt/v solution of Alginate in chloroform was prepared, the nanopowders were added, and the mixture was stirred for 12 h till a well-dispersed homogenous suspension was obtained. The suspension was frozen at –80 °C during 24 h to induce the solid–liquid phase separation of the polymer solution. The solvent was extracted from the frozen sol–gel nanopowders/ polymer mass by immersion into absolute ethanol at –80 °C, and ethanol was replaced with fresh ethanol each 8 h during two days. After complete extraction of chloroform, ethanol was removed by drying at room temperature to obtain the porous scaffolds.[23]

2.3. Characterization

The phase analysis of the samples was examined by X-Ray diffractometer (Diana Corporation, USA) equipped with CoK radiation. The FT-IR spectra measured using KBr pellets made from a mixture of the powder for each sample and assessed from 400 to 4000 cm^{-1} using a Nexus 670, Nicloet FT-IR spectrometer, USA. SEM micrographs of the composites were also studied using SEM Model Philips XL 30, with accelerating voltage 30KV.

The test microorganism was *Staphylococcus aureus*. Antibacterial test has been carried out as follows: 40 ml of the agar medium inoculated with 200 micro liter of the test microorganism prepared inoculums and poured in 15 cm diameter Petri dish and solidified. After placing the disks of the tested materials on the surface of the solidified agar and let it to diffuse in the medium, the plate was incubated at 37°C for 24 hours. The observation of the Halo zones was carried out to assess the antimicrobial activity.

The composites were tested to determine the effect of polymeric matrix on the mechanical properties of the composites. The average value for each test was taken for ten readings to confirm the results. The compressive strength was measured for the prepared composites by using tensile testing machine, Zwick Z010, Germany. The average value for each test was taken for three samples to verify the results. The shape of sample was cylindrical (1 cm \times 2 cm), load cell was 10 KN and crosshead speed was 10 mm/min.

The SBF has a composition similar to human blood plasma and has been extensively used for in vitro bioactivity test. After immersion for 21 days, the specimens were removed from the SBF solution and were abundantly rinsed with deionized distilled water in order to remove the soluble inorganic salts and to stop the reaction. FT-IR analysis was also carried out for the samples pre- and post-immersion to confirm the formation of apatite layer onto the surface. The surfaces of samples were also analyzed pre- and post-immersion for 21 days in SBF using scanning electron microscope Fourier transform infrared spectrometer (SEM) coupled with energy dispersive X-ray analysis (SEM/EDX) to determine the calcium/phosphorus ratio for surface apatite onto the copolymer and composite samples. For SEM, the substrates were mounted on metal stubs and coated with carbon before examination.

RESULTS AND DISCUSSION

3.1. Scanning electron microscope (SEM) of multi-wall carbon nanotubes (MWNT)

Figure (1), shows the representative scanning electron microscopy (SEM) image of MWCNT alone. It indicates that the product is composed of nanostructures. The diameter of the MWCNT is between 95.5 nm and 196 nm, as shown in Figure 1.

3.2. X-Ray diffraction analysis

Figure (2), shows the XRD patterns of Alginate polymer alone (a), HA/Alginate composite (b), HA/ZnO/Alginate composite (c) and HA/ZnO/ MWCNT / Alginate composite (d), respectively.

The XRD pattern of Alginate polymer alone obtained an amorphous structure. No specific peaks were observed in pure alginate, indicating an amorphous-like structure. The XRD pattern of HA/Alginate composite obtained the characters peaks of hydroxyapatite structure 2θ ; 31.7°,

32.9° and 32.1°. These features corresponded well to those expected from the hydroxyapatite structure.



Fig(1): SEM image of multi-walled carbon nanotube MWCNT.

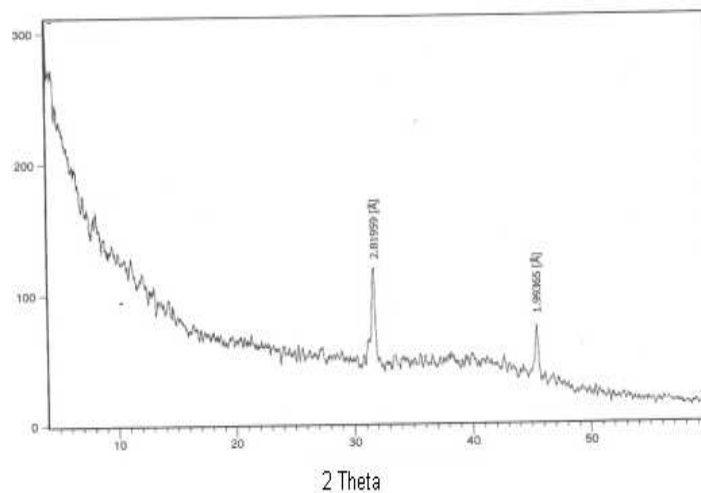


Fig.(2.a.) :XRD of Alginate polymer matrix alone.

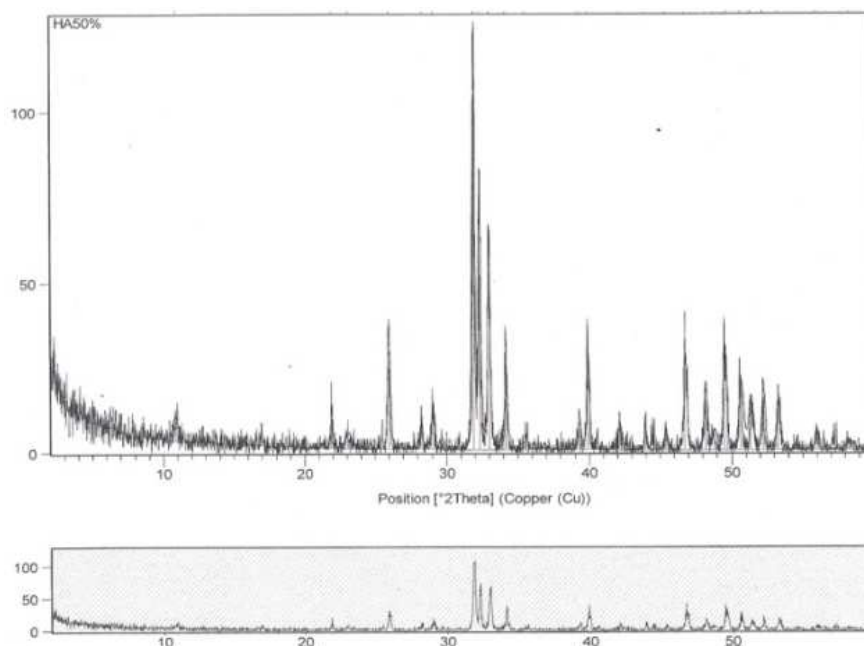


Fig.(2.b.) XRD of HA/Alginate composite.

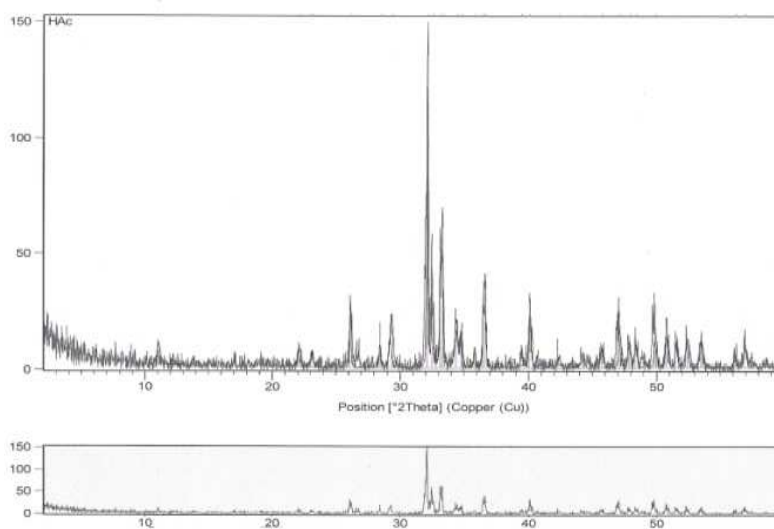


Fig.(2.c.) XRD of HA/ ZnO/ Alginate composite.

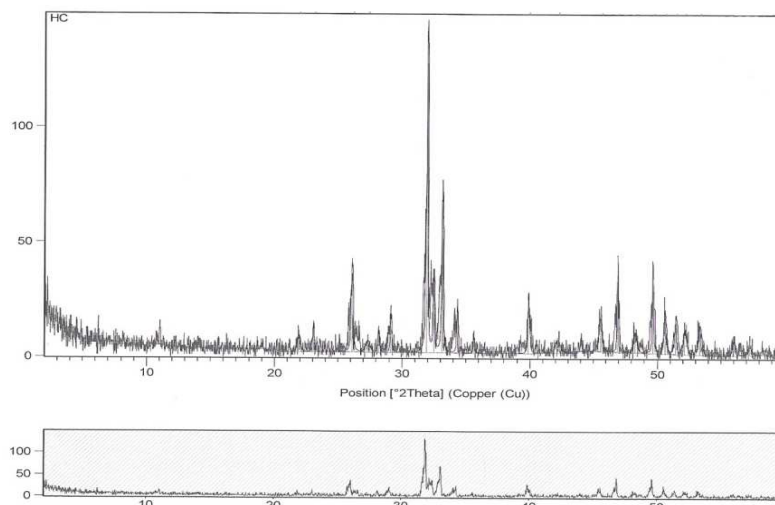


Fig.(2.d.) XRD of HA/ ZnO/ MWCNT/Alginate composite.

The characteristics of the crystal structure of hydroxyapatite tended to be some unclear in Alginate composite as compared with the pure hydroxyapatite. Fig. (2 - c) shows the XRD pattern of HA/ZnO/Alginate composite obtained the characters many peaks of hydroxyapatite structure beside the peaks of ZnO. Fig.(2 - d) shows the XRD pattern of HA/ZnO/ MWCNT /Alginate composite obtained the characters of some peaks of hydroxyapatite structure beside the peaks of ZnO and MWCNT obtained from X-ray diffraction data are consistent with the JCPDS data of hydroxyapatite, ZnO and MWCNT. There is a little shift of peaks due to the alginate polymer.

3.3. Fourier transmitter infra spectroscopic analysis of nano-composites before in-vitro study

Figure (3), shows the FT-IR spectra of Alginate polymer alone (a), HA/Alginate composite (b), HA/ZnO/Alginate composite (c) and HA/ZnO/ MWCNT /Alginate composite (d). Three distinct bands originating from ν_3 P-O in the orthophosphate stretch absorption around 1030–1130 cm^{-1} and PO_4^{3-} bands at 906 and 1100 cm^{-1} typical of the hydroxyapatite structure were observed in the spectra of the composites (b–d) except the spectrum of the original Alginate polymer alone. Two sharp absorption bands of group PO_4^{3-} at 560–600 cm^{-1} were ascribed to crystalline calcium phosphate. It was hard to detect differences among alginate spectra, it shows large absorbance at the wave numbers where peaks due to amide bonds and silanol groups appear. The 1620 and 1416 cm^{-1} bands are assigned to the anti-symmetric and symmetric COO-stretching vibration of the carboxyl group of alginic acid, respectively. The intensity of these bands assigned to alginate decreased with decreasing the hydroxyapatite ratio in the composites. The bands of PO_4^{3-} region (1000–1200 cm^{-1}) of the hydroxyapatite structure became broader in the spectra of the composites. In both XRD and FT-IR results, the characteristic peaks of hydroxyapatite were maintained in the composites, suggesting that the alginate did not induce subsequent modifications in the crystal structure of hydroxyapatite.

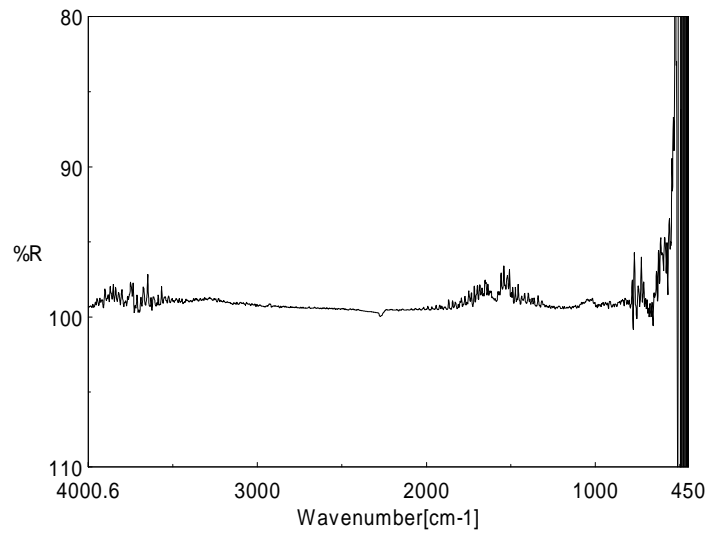


Fig.(3.a.) :FTIR o f Alginate polymer alone before in- Vitro test.

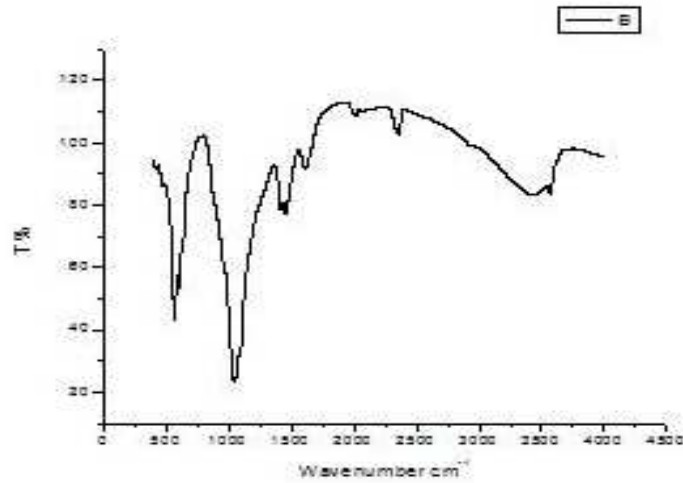
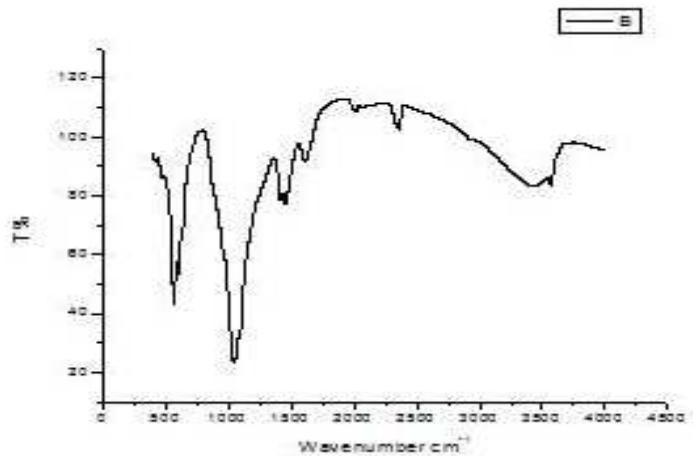


Fig.(3.b.) :FTIR o f nano-HA/ Alginate composite before in- Vitro test.



.(3.c.) :FTIR o f nano-HA/ZnO/ Alginate composite before in- Vitro test.

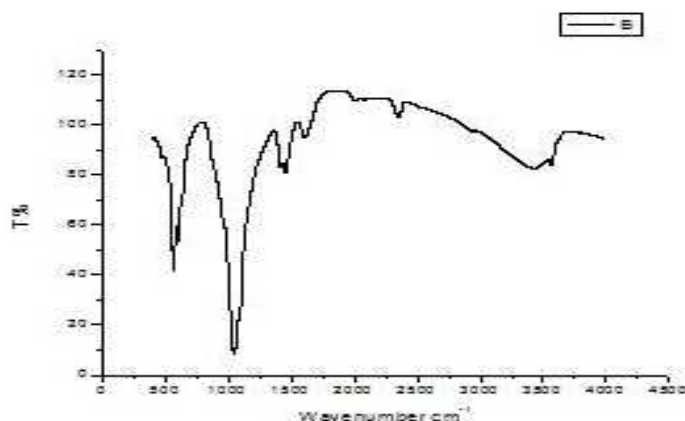
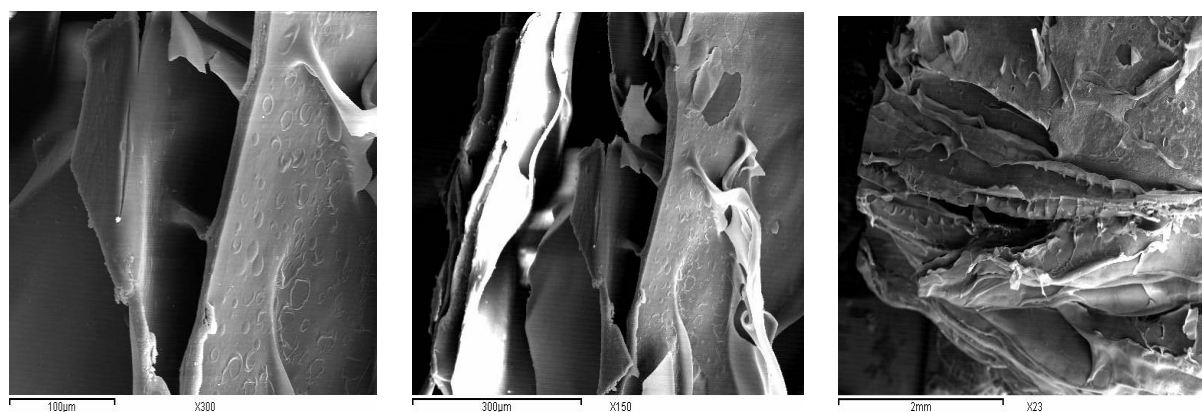


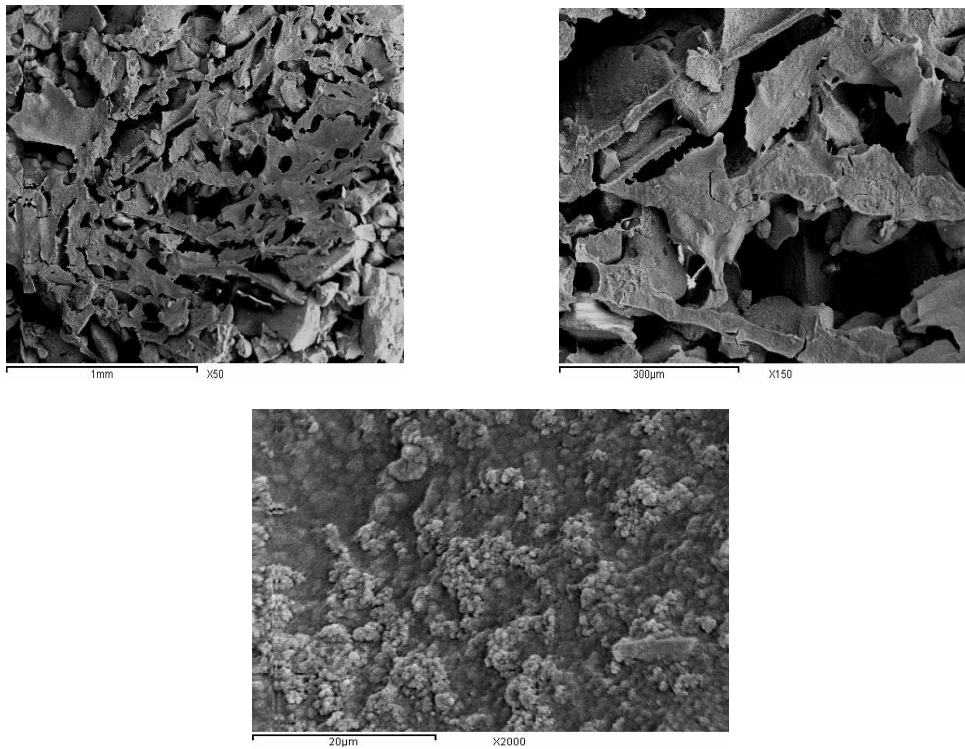
Fig.(3.d.) :FTIR of nano-HA/ZnO/ MWCNT /Alginate composite before in-Vitro test.

3.4. SEM of nano-composites before In-Vitro study

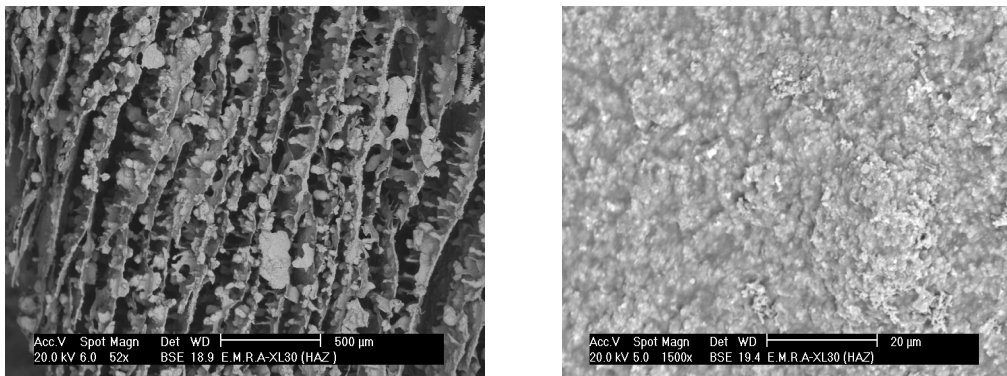
Figure (4), shows SEM micrographs of Alginate polymer alone (a), HA/Alginate composite (b), HA/ZnO/Alginate composite (c) and HA/ZnO/ MWCNT /Alginate composite (d). SEM micrographs of Alginate polymer alone was highly porous and had a well-interconnected pore structure (Fig. 4 - a). In higher magnification, Alginate polymer alone exhibited smooth surfaces with a sheet-like morphology low porous, well-interconnected pore structure was also observed in the HA/Alginate composite (Fig. 4 - b), although the pore size of the composites was clearly different from that of Alginate polymer alone. In the HA/ZnO/Alginate composite, hydroxyapatite and ZnO crystals were partially embedded within the Alginate matrix throughout the walls (Fig. 4-c). Fig.(4-d) shows the macrostructure of HA/ZnO/ MWCNT /Alginate composite. On the other hand, in the composites, hydroxyapatite crystals were observed as a plate like morphology about 2–5 μm in length on the surface as well as the inner walls of the scaffolds. The surfaces of the composites were rough, and nanopowder crystals were homogeneously dispersed in the polymer matrix. Figure 4 shows that the porous structure is comprised of large macropores with diameters in the region of 200–600 μm that is highly interconnected. Many of the interconnect apertures (dark areas) have diameters in excess of the 100 μm required for tissue engineering application.



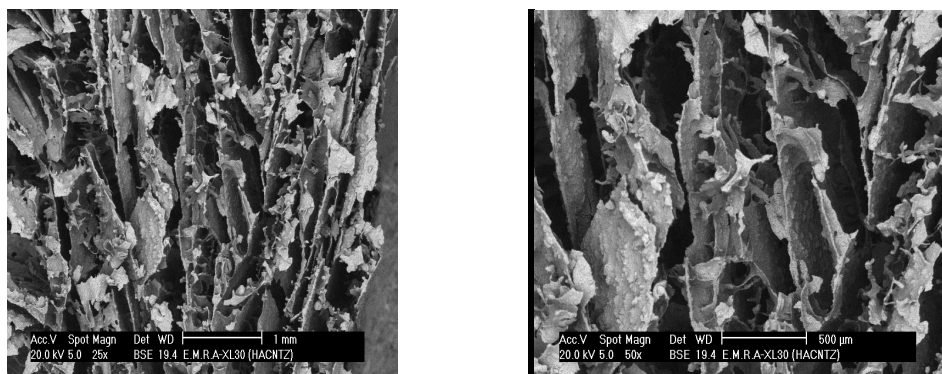
Fig(4.a.) :SEM of Alginate polymer alone before in- Vitro test.

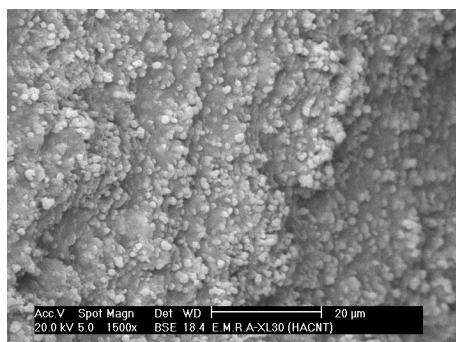


Fig(4.b.) : SEM of nano-HA/ Alginate composite before in- Vitro test.



Fig(4.c.) : SEM of nano-HA/ZnO/ Alginate composite before in- Vitro test.





Fig(4.d.) : SEM of nano-HA/ZnO/MWCNT/Alginate composite before in- Vitro test

3.5. Pore analysis

The interconnected pore aperture distributions were obtained from mercury intrusion porosimetry (Table 1). Table 1 shows that scaffolds that were formed with 90.97% porosity and exhibited a modal interconnected pore diameter of $70\mu\text{m}$ for Alginate polymer alone. The reduced modal pore diameter decreased to $60\mu\text{m}$ and porosity to 86.34% for HA/Alginate composite. $100\mu\text{m}$ should be a suitable pore size for tissue engineering applications as there appears to be many apertures larger than the mode. From Table 1, the pore characters decrease for HA/ZnO/Alginate composite and HA/ZnO/MWCNT/Alginate composite.

The bimodal distribution was caused by being insufficient in the surface tension of the sol to a level that would create a homogeneous distribution of pores. Scaffolds produced with these porosities are unlikely to be useful in tissue engineering applications.

Table (1) :The pore analyses of Nano-powders/ Alginate

Sample	Total pore area (m ² /g)	Av.Pore diameter(um)	Bulk density(g/ml)	Apparent density (g/ml)	Total porosity (%)
Alginate	104	70	1.11	5.86	80.97
HA/Alginate	96	60	1.4	3.86	86.34
HA/ ZnO /Alginate	84	65	1.2	3.6	83.98
HA/ZnO/MWCNT/Alginate	75	40	1.3	3.15	80.97

3.6. Mechanical properties

Table (2), shows the compressive strength of the prepared composites. The compression test of the composites increased with the increase of the composite which includes MWCNT. These results demonstrated that the mechanical properties of porous scaffolds were significantly affected by adding the MWCNT in the composite.

Despite the fact that the porosity of all the composites remained nearly constant and the pore size of all composites was larger than that of Alginate alone, this may be due to an increase in the pore wall thickness and the density of these composites.

Table (2) :The mechanical properties of nano-powders / Aginate composites

Composites	Alginate	HA/Alginate	HA/ZnO/Alginate	HA/ZnO/CNT/Alginate
Compressive strength (MPa)	4	6	9	24

3.7. Fourier transmitter infrared analysis of nanocomposites after in-vitro study (FT-IR)

Standard in-vitro bioactivity tests were carried out to evaluate whether or not the apatite layer on the surface of nano-composites was formed as an indicator for the in- vivo bioactivity of the nano-composites. Figure (5), shows the FT-IR spectra (after in-vitro study) of Alginate polymer alone (a), HA/Alginate composite (b), HA/ZnO/Alginate composite (c) and HA/ZnO/ MWCNT /Alginate composite (d).The optical density (O.D.) of the Alginate polymer alone peaks such as OH at 3428 cm^{-1} , phosphate overlapping with C-H at 749 and 905 cm^{-1} and phosphate overlapping with C-O at 1070 and 1160 cm^{-1} are enhanced post-immersion compared to pre-immersion proving mineralization of phosphate ions from SBF. This result is in favor of the formation of the apatite layer. For HA/Alginate composite, Fig.5 shows that the O.D. of OH at 2950 and 3450 cm^{-1} and phosphate groups at 470 and 1070 cm^{-1} into the spectra of three composites are enhanced post-immersion compared to pre-immersion after 21 days proving mineralization of phosphate ions onto the surface. For HA/ZnO/Alginate composite, new peaks appeared at 805 , 880 and 1440 cm^{-1} which are assigned to carbonate group's post-immersion proving formation of carbonated apatite layer. For HA/ZnO/ MWCNT /Alginate composite, new bands appeared such as phosphate band at 910 cm^{-1} and carbonate groups at 1400 - 1470 cm^{-1} denoting formation of carbonated apatite layer. Also, for HA/ZnO/ MWCNT /Alginate composite, new peaks appeared of carbonate groups at 1460 cm^{-1} denoting formation of carbonated apatite layer. [24 and 25] Also, the polymer bands such as OH, C=O, O-C-C-O, C-O and CH in the spectra of the three composites had enhanced O.D. post-immersion compared to pre-immersion in SBF indicating their involvement in the structure of bio-layer. Additionally, it is noted that the three composites had ability to form the carbonated apatite layer onto their surfaces (Fig.5).

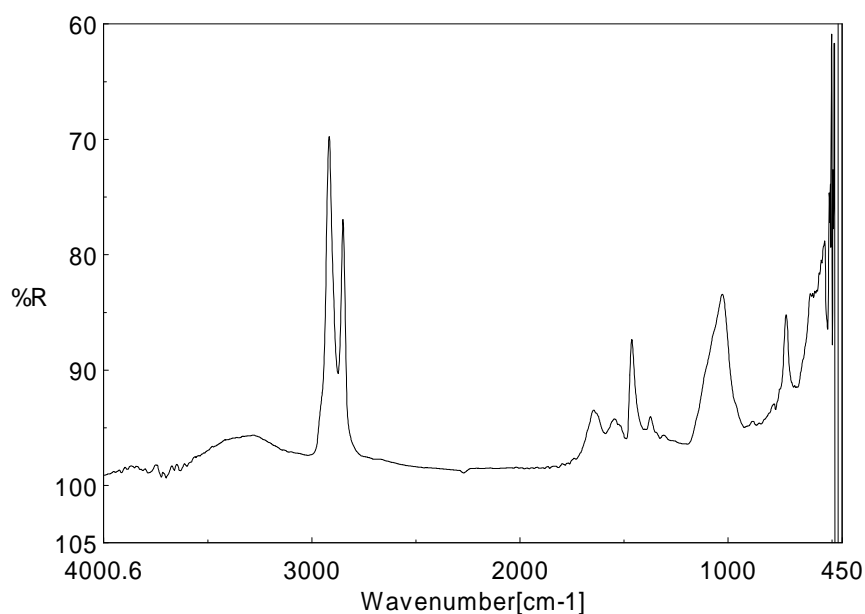
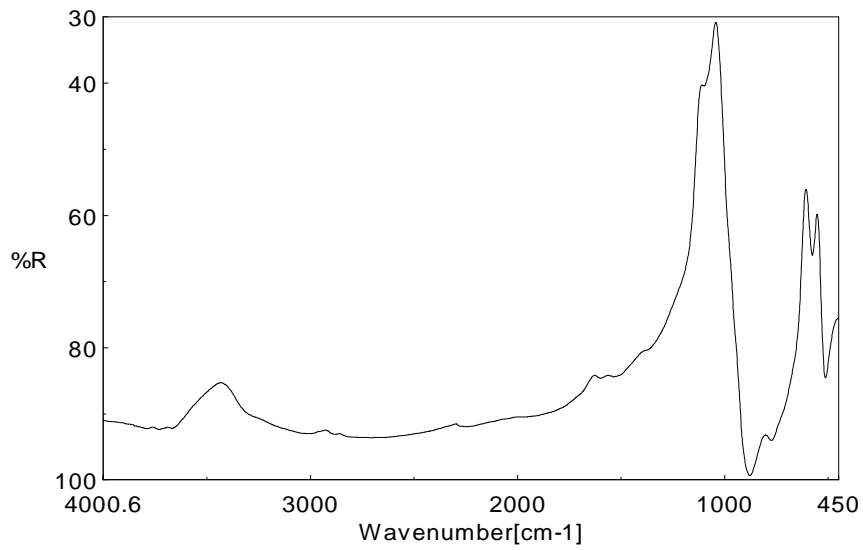


Fig.(5.a.) : FTIR of Alginate polymer after in- Vitro test.



Fig(5.b.) :FTIR o f nano-HA/ Alginate composite after in- Vitro test.

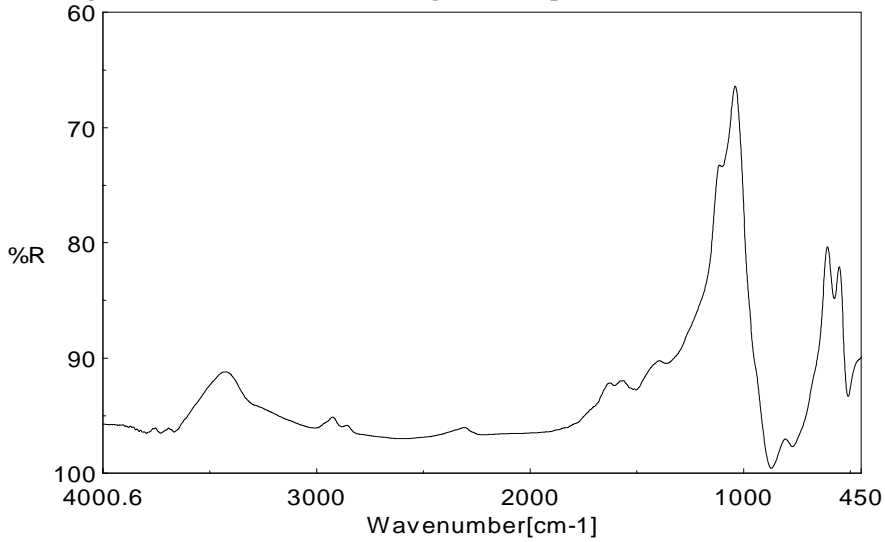


Fig (5.c.) :FTIR o f nano-HA/ZnO/ Alginate composite after in- Vitro test.

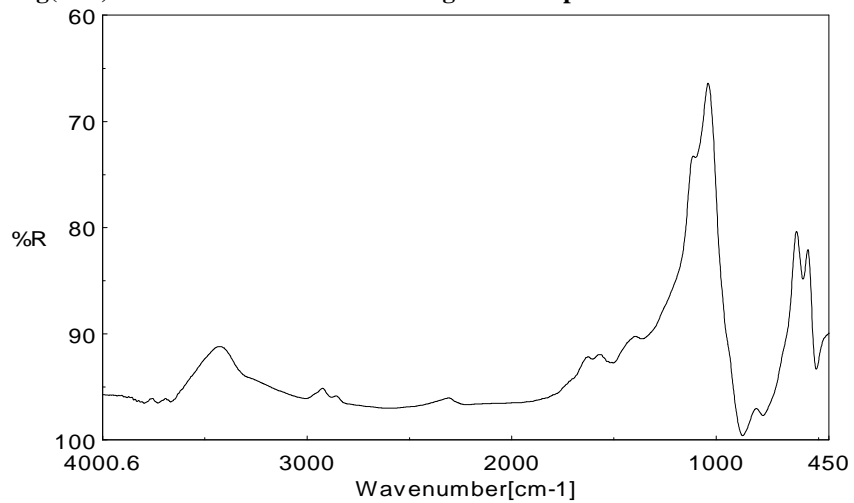


Fig (5.d.) :FTIR o f nano-HA/ZnO/MWCNT/Alginate composite before in- Vitro test.

3.8. SEM of nano-composites after in-vitro study

SEM micrographs of the surface of the neat polymer alone (Alginate) and the composites, after immersion in the SBF for 21 days, are shown in Fig.6. This figure also shows the EDX analysis of the sample's surfaces. For the neat polymer scaffold Alginate it was previously reported that it could induce the development of the apatite layer on its surface after soaking in the SBF. However, in our study, apatite was formed even after immersion in SBF for 21 days (Fig. 6) as also confirmed by the EDX analysis of the surface of composites that showed that the main elements were, Ca, P, carbon and oxygen [26 and 27]. A small amount of calcium and phosphorus was found after soaking in SBF for 21 days (Alginate alone). On the other hand, a layer of spherical particles fully covered the surfaces of all composites especially the composites which include MWCNT. The EDAX analysis in these figures suggested that these spherical particles could be calcium-deficient and non-stoichiometric apatite with Ca/P ratio of 1.56 and 1.64 for HA/Alginate composite and HA/ZnO/Alginate composite respectively. This ratio is close to that of natural apatite in bone. Other studies have reported that the induced apatite layer on the surfaces of different bioactive materials during their incubation in SBF was also calcium-deficient.[28] The formation of the hydroxyapatite layer on the surface of composite scaffolds, immersed in SBF, could be explained by the hydrolysis of ester bonds of the polymer, and the formation of carboxylate groups (COOH). These reactive groups have the ability to attract PO₄ group released from the scaffolds due to the dissolution of the nano-HA particles. [28 -30]

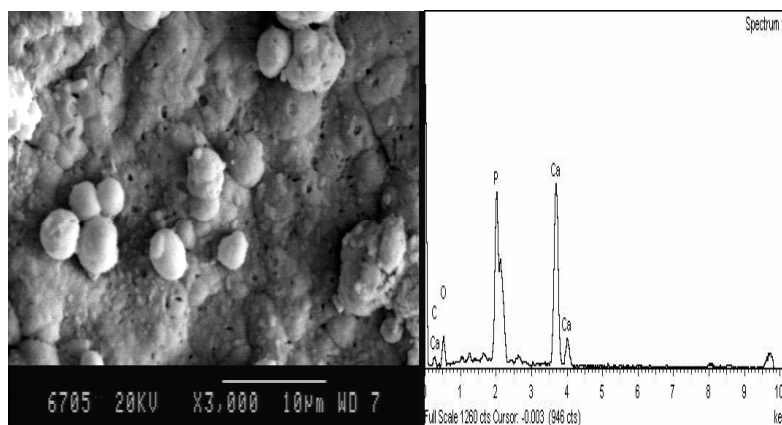


Fig (6.a): SEM and EDX of Alginate polymer alone after in- Vitro test.

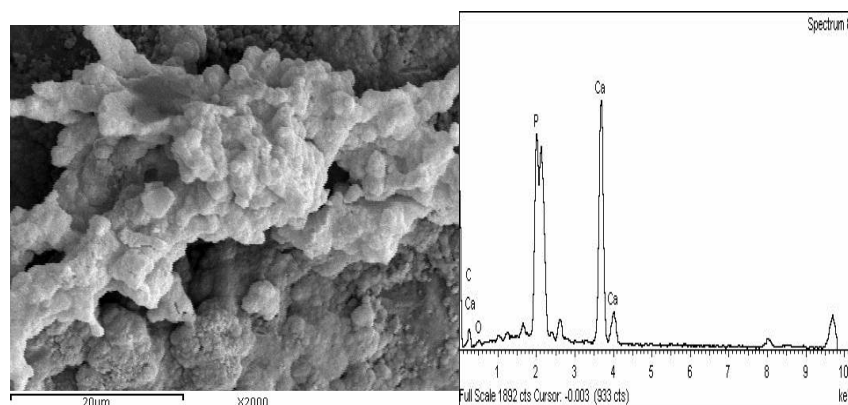


Fig. (6.b.) : SEM and EDX of nano-HA/ Alginate composite after in- Vitro test.

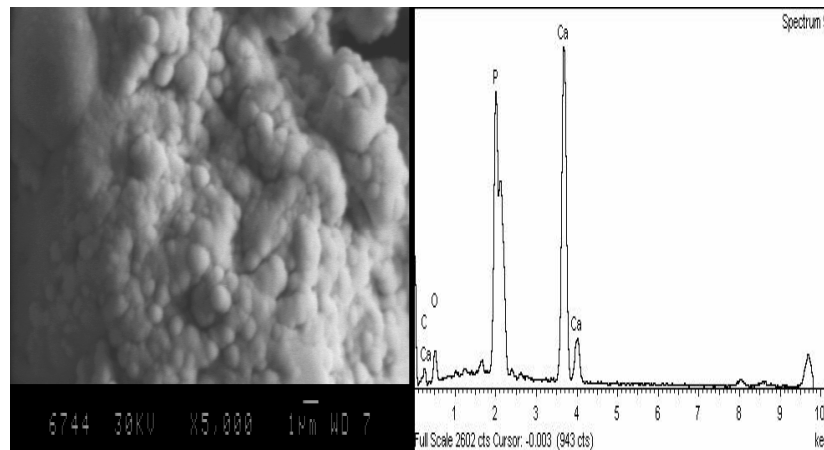
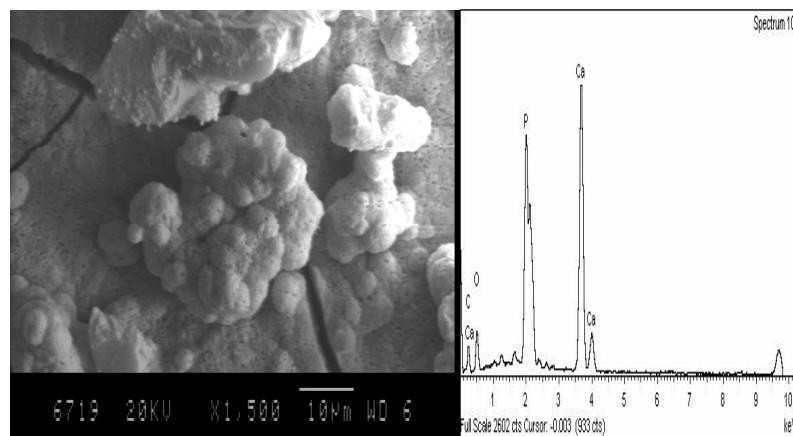


Fig (6.c.): SEM and EDX of nano-HA/ZnO/ Alginate composite after in- Vitro test.



Fig(6.d.): SEM and EDX of nano-HA/ZnO/MWCNT /Alginate composite after in- Vitro test.

The agar culture medium is transparent. The test microorganism culture is colored. When the bacterium is inhibited from growth, a transparent area in the form of a halo around the disk was observed Zhang *et.al.* [27]. The antibacterial test results for the HA/ ZnO/ Alginate composite and HA/ ZnO/ MWCNT /Alginate composite only.

CONCLUSION

The design requirements for the scaffolds for bone tissue engineering may include biocompatibility, controlled degradability, mechanical integrity, vascularization inductivity, excellent bone guidance, osteoconductivity, and osteoinductivity. Biomaterials containing polymers have some of the above features, and they may lack few of them (for example, mechanical integrity). MWCNT possess exceptional mechanical, thermal, and electrical properties, facilitating their use as reinforcements or additives in various biomaterials to improve the properties of the biomaterials and to support osteoblastic cell growth and differentiation.

The XRD, SEM, antimicrobial test and FT-IR results confirmed that the prepared antimicrobial and bioactive composites containing novel nano-powders into the Alginate polymer matrix had enhanced apatite coating onto the surface of the all composites. Compressive strength of the composites had values comparable to those of cancellous bone. In vitro test results via calcium and phosphate ions measurements confirmed that the composite had slightly enhanced ability to accelerate the mineralization of calcium phosphate layer on its surface compared to Alginate alone polymer surface proving the vital role of Alginate polymer in the mineralization process. FT-IR and SEM provided by EDX post-immersion confirmed that polymeric composites lead to the formation of apatite onto their surfaces especially this composite containing MWCNT matrix. Finally, novel biocomposites having bioactivity properties could be used in bone substitutes and tissue engineering applications.

REFERENCES

- [1] T.S. Einhorn, *J. Bone. Surg.*, **1995**, 77, 940–56.
- [2] T. Kokubo, H. Kushitani, Y. Abe, T. Yamamuro, In: Heimke G., editor *Bioceramics*. Vol. 2 German Ceramic Society, **1990**, 2, 235–242.
- [3] R. Verdejo, G. Jell, L. Safinia, A. Bismarck, M. Stevens, P. Shaffer, *J. Biomed. Mater. Res.*, **2009**, A 88 , 65–73.
- [4] D. Lickorish, J. Ramshaw, J. Werkmeister, V. Glattauer and C. Howlett, *J. Biomed. Matziner. Res.*, **2004**, 68A, 19–27.
- [5] A. Ciftecioglu, N. Yamaguchi, K. Tokuchi, H H . Fukuzaki, Y.Koyama, K. Takakuda and H. Tanaka, *Biomaterials.*, **2003**, 24, 3991-3998.
- [6] A. Nayak and A. Dhara, *Archives of Applied Science Research*, **2010**, 2 (2), 284-293.
- [7] W. Chen, Y. Liu, H. Courtney, M. Bettenga, C. Agrawal, J. Bumgardner and J. Ong, *Biomaterials*. **2006**, 27, 5512–5517.
- [8] A. Peigney, C. Laurent and O. Dumortier, *J. European Ceramic Society.*, **2004**,18, 1995–1998.
- [9] K. Tak Lau and D. Hui, *Carbon.*, **2002**, 40, 1597–1617.
- [10] A. Kumar and Doshi H. et.al *Polymer.* ,**2002**,43, 1701–1703
- [11] K. Balania, R. Andersonb, T. Lahaa, M. Andaraa , J. Terceroa, E. Crumplerb and A. Agarwala, *Biomaterials*. **2007**, 28, 618–62.
- [12] B. Harrison and A. Atala , *Biomaterials.*,**2007**, 28, 344–353.
- [13] M. Erstan and C. Bucke, *Biotechnol. Bioeng.*,**1977**,19, 387.
- [14] M. Confalonieri and E.Damonti , *GIMMOC .*, **2003**, 1, 21–26.
- [15] D. Campoccia, L. Montanaro and C. Arciola, *Biomaterials*. **2006**, 27, 2331–2339.
- [16] A. Kumar and P. Schweizer, *Adv. Drug Deliv. Rev.*, **2005**, 57, 1486–1513.
- [17] S. Di Nunzio, C.Vitale Brovarone , S. Spriano, D. Milanese, E. Vern´e, V. Bergo, G.Maina and P.Spinelli, *J. Eur. Ceram. Soc.*, **2004**, 24, 2935–2942.
- [18] L. Zhao, E. Burguera, H. Xu, N. Amin, H. Ryou, and D. Arola, *Biomaterials*, **2010**, 31, 840–847.
- [20] S. Smart, A. Cassady, G .Lu and D. Martin, *Carbon.*, **2006**, 44, 1034–1047.
- [21] H. Beherei, A. El-Magharby and M. Selim, Under press in *Ceramic Int.*(**2011**).
- [22] H. Beherei, A. El-Magharby and M. Selim, Under press in *Nano-Powder J.*(**2011**).
- [23] P.X. Ma, *Materials Today.*, **2004**, 7 (5) , 30.

- [24] N. Binulal, M. Deepthy, N. Selvamurugan, K. Shalumon, S. Suja, U. Mony, R. kumar and S. Nair, *Tissue Engineering Part A*. **2010**, 16(2), 393-404.
- [25] H. Meng, L. Chen, Y. Zhaoyang, S. Wang and X. Zhao, *J. Biomed. Mater. Res. B: Appl. Biomaterials.* , **2009**, 89B379-391.
- [26] J. Jones, L. Ehrenfried, P. Saravanapavan, L. Hench, *J. Mater. Sci: Mater. Med.*, **2006**,17, 989–996.
- [27] T. Theivasanthi and M. Alagar, *Annals of Biological Research*, **2011**, 2 (3) , 82-87.
- [28] A. Abarrategi, C. Gutierrez, H. Moreno, C. Vicente et al., *Biomaterials*. **2008**, 29, 94 – 102.
- [29] M. Tanahashi, T. Kokubo, T. Nakamura, Y. Katsura and M. Nagano, *Biomaterials.*, **1996**, 17, 47–51.
- [30] X. Shi, B. Sitharaman, Q. Pham, P. Spicer, J. Hudson, L. Wilson, J. Tour, R. Raphael and A. Mikos, *J. Biomed. Mater. Res.*, **2008**, A 86 , 813–823.